

Oxygen transfer in a gas–liquid system containing solids of varying oxygen affinity

Jennifer V. Littlejohns, Andrew J. Daugulis*

Department of Chemical Engineering, Queen's University, Kingston, Ontario K7L 3N6, Canada

Received 5 September 2006; received in revised form 25 October 2006; accepted 8 November 2006

Abstract

An air sparged, mechanically agitated bioreactor containing spherical solids was studied in order to determine the effect of the solid phase on oxygen mass transfer. It was found that both nylon 6,6 and glass beads cause an enhancement of the volumetric mass transfer coefficient of up to 268%, whereas particles of silicone rubber and styrene–butadiene copolymer reduce the volumetric mass transfer coefficient by up to 63%, relative to a system without a solid phase. A simple transport in series model has been proposed to account for the observed phenomena, which includes both the physical enhancement effects of particles on gas–liquid mass transfer as well as absorption of oxygen into the polymer. Even though volumetric mass transfer coefficient reductions were observed in the system containing silicone rubber, it was demonstrated that an increased oxygen transfer rate into the working volume of a two-phase system occurs relative to a system without a solid phase. This study provides an explanation for previous results regarding the enhanced effect of the presence of a styrene–butadiene copolymer phase in reducing oxygen limitations in a solid–liquid two-phase partitioning bioreactor. Results from this study can be applied to two-phase aerobic fermentation systems that will benefit from reducing oxygen limiting conditions.

© 2006 Elsevier B.V. All rights reserved.

Keywords: Oxygen transfer rate; $k_L a$; Solid–liquid two-phase partitioning bioreactor

1. Introduction

The limiting rate in many aerobic bioreactor systems is the transport of oxygen from the gaseous phase to the liquid phase due to the low solubility of oxygen in water. As a result, the volumetric mass transfer coefficient, $k_L a$, is often quantified in order to allow for proper system design. However, the presence of a third phase can have a large impact on $k_L a$, which must be accounted for in order to ensure that the system is not oxygen limited, nor over designed. Liquid–liquid two-phase partitioning bioreactors (TPPBs), which consist of a working volume of two-phases treating a contaminated gaseous phase, have been shown to ease oxygen limitations by the presence of immiscible organic solvents such as *n*-hexadecane. Due to a larger oxygen concentration in the liquid–solvent phase at equilibrium with the gaseous phase, the overall mass transfer rate of oxygen into the liquid–liquid system is increased according to a larger gas–liquid driving force [1]. However, this causes the mea-

sured volumetric mass transfer coefficient to be lower relative to the absence of a second liquid phase due to the system taking longer to reach the higher saturation value. The measured volumetric mass transfer coefficient for a system consisting of two distinct phases in the working volume with significant oxygen affinity is defined as the effective volumetric mass transfer coefficient, $k_L a_{\text{eff}}$. The presence of solid styrene–butadiene copolymer beads in a solid–liquid TPPB has also been found to reduce oxygen limitations in comparison to a system without a second solid phase that encountered oxygen limitations under the same conditions as the solid–liquid TPPB [2]. As a result of these findings, there is an interest in quantifying the effect of polymer beads in a TPPB on oxygen mass transfer.

Many studies have been completed regarding the effect of solid particles on gas–liquid oxygen mass transfer but a simple mechanism to describe all cases does not exist. Some systems show an enhanced $k_L a$ [3–5] and some systems measure a decreased $k_L a$ [6,7] relative to systems without particles. It is clear, however, that the effect of the particles on the system is a function of particle properties, vessel and impeller dimensions and arrangement and operating conditions [8,9]. Such particle properties include oxygen diffusivity of the solid particles [10],

* Corresponding author. Tel.: +1 613 533 2784; fax: +1 613 533 6637.
E-mail address: andrew.daugulis@chee.queensu.ca (A.J. Daugulis).

Nomenclature

C_L	concentration of oxygen in the liquid phase (mg/L)
C_p	concentration of oxygen in the liquid phase read by the oxygen probe (mg/L)
C_S	concentration of oxygen in the polymer phase (mg/L)
C_{sys}	concentration of oxygen in the working volume (mg/L)
C^*	concentration of oxygen in the liquid phase in equilibrium with the gas phase (mg/L)
E_p	physical enhancement factor
$k_{L a_{\text{eff}}}$	the gas–liquid effective volumetric mass transfer coefficient, for systems with absorptive particles (h^{-1})
$k_{L a_{\text{INERT}}}$	the gas–liquid inert volumetric mass transfer coefficient, for systems with inert particles (h^{-1})
$k_{L a}$	the gas–liquid inert volumetric mass transfer coefficient, for systems without particles (h^{-1})
V_L	volume of the liquid phase (L)
V_S	volume of the polymer phase (L)
<i>Greek symbol</i>	
τ_p	time constant for the DO probe response (h^{-1})

particle density [6,11], particle size [7,12], particle hydrophobicity [13], and concentration of particles [9,14].

Enhancement of $k_{L a}$ was observed for small particles present in gas–liquid systems and this was originally explained to be due to a shuttling effect wherein absorptive particles enter the liquid boundary layer, absorbing dissolved gas and then desorbing the dissolved gas when back in the bulk phase [15]. Shuttling has been shown to be predominant in particles with a size equal or smaller than the gas–liquid boundary layer [15,16], however, this size is much smaller than that used in a solid–liquid TPPB. It has also been shown that enhancement can occur in systems with inert particles, i.e. without absorptive properties, which indicates that there are several mechanisms acting on a gas–liquid–solid system to increase the gas–liquid mass transfer [3]. The possible mechanisms that can account for this phenomenon include boundary layer mixing and changes in interfacial area. Boundary layer mixing involves an increase in k_L due to turbulence at the gas–liquid interface [10,16], which causes a larger refreshment rate of liquid in the boundary layer by mixing with the bulk fluid. Changes in the gas–liquid interfacial area can be caused by particles being present at the gas–liquid interface, causing coalescence inhibition and an increase in ‘ a ’ [16].

The purpose of this investigation was to determine $k_{L a_{\text{eff}}}$ in an abiotic solid–liquid TPPB system for various solid types. This will be compared to $k_{L a_{\text{INERT}}}$, which is defined as the measured volumetric mass transfer coefficient of a system containing two distinct phases, with the solid phase having negligible oxygen affinity (inert). As well, both $k_{L a_{\text{eff}}}$ and $k_{L a_{\text{INERT}}}$ were compared to a single aqueous phase, $k_{L a}$. A

theoretical “transport in series” model was developed involving an estimated physical enhancement term in order to determine the oxygen uptake by the polymer beads. Finally the increased oxygen transfer rate in a solid–liquid TPPB relative to a system without a second phase was demonstrated.

2. Materials and methods

2.1. Volumetric mass transfer coefficient

The bioreactor used was a New Brunswick Bioflo™ III with an internal diameter of 17 cm, which was agitated by a single six blade Rushton turbine impeller of diameter 7.7 cm. Four baffles were also provided to increase mixing. All experiments were operated at 30 ± 0.1 °C, and measurements were taken in duplicate with the average value being reported.

All systems, which consisted of 500 g of each solid type in tap water to total working volume of 3 L, were operated at aeration rates of 0.5 L/min, 0.75 L/min and 1 L/min. This was repeated for agitation rates of 100, 200, 300 and 400 rpm, with the exception of glass beads, which was only stirred at 400 rpm due to the inability to suspend the glass beads at lower agitation rates. Higher operating conditions of 1, 2, and 3 L/min for each of 400, 600 and 800 rpm were also completed for each system.

Using three different polymer types, nylon 6,6, styrene–butadiene copolymer and silicone rubber, with properties listed in Table 1, $k_{L a_{\text{eff}}}$ was determined. As well, $k_{L a_{\text{INERT}}}$ was determined using glass beads, with properties also listed in Table 1. All solid particles used were approximately spherical in shape. Styrene–butadiene copolymer and nylon 6,6 were obtained from Scientific Polymer Products, Inc., glass beads were obtained from Fisher Scientific and silicone rubber was obtained from GE-Mastercraft® in the form of 100% silicone rubber caulking. The caulking was dried to spherically shaped beads.

The unsteady-state method was used to determine $k_{L a_{\text{eff}}}$, $k_{L a_{\text{INERT}}}$ and $k_{L a}$ as described by Shuler and Kargi [17]. The system was first sparged with nitrogen in order to remove oxygen. Air was then delivered into the reactor through a 5 mm diameter single orifice sparger that was directly below the mechanical agitator and located 1.5 cm from the bottom of the tank. Oxygen concentration was measured by an OxyProbe® D100 Series Polarographic Dissolved Oxygen (DO) Sensor (Broadley James Corp.) until saturation was reached. For consistency, data between 30% and 80% of liquid saturation were used for the determination of $k_{L a_{\text{eff}}}$, $k_{L a_{\text{INERT}}}$ and $k_{L a}$. An integrated, linearized form of Eq. (1) can then be utilized in order to determine $k_{L a_{\text{eff}}}$, $k_{L a_{\text{INERT}}}$ and $k_{L a}$, which is the negative slope of the log of the concentration driving force versus time.

$$\begin{aligned} \frac{dC_L}{dt} &= k_{L a}(C^* - C_L) \text{ or } \frac{dC}{dt} = k_{L a_{\text{eff}}}(C^* - C_L) \text{ or } \frac{dC}{dt} \\ &= k_{L a_{\text{INERT}}}(C^* - C_L) \end{aligned} \quad (1)$$

Under circumstances in which low aeration and agitation rates were used, surface aeration for this reactor could have been significant, but it was found (data not shown) that the mass

Table 1
Properties of solids

Polymer	Oxygen diffusivity (cm ² /s)	Diameter (mm)	Density (g/L)
Nylon 6,6	1.6×10^{-9} [23]	2.59	1140
Styrene–butadiene copolymer	1.4×10^{-6} [24] ^a	3.57	940
Silicone rubber	3.4×10^{-5} [25] ^b	2.5	1150
Glass	$<10 \times 10^{-16}$ [26]	6	2500

^a Butadiene/styrene (wt:wt parts%) 77:23 This is an approximation, as the styrene–butadiene used in this study was butadiene/styrene (wt:wt parts%) 72:28.

^b Value measured at 35 °C.

transfer coefficients due to surface aeration are negligible in comparison to those found with gas sparging and agitation.

There is a significant response time lag between the actual percent saturation of oxygen in the water and that which is read by the oxygen probe if the time constant of the probe, τ_p , is much smaller than the inverse of $k_L a_{\text{eff}}$, $k_L a_{\text{INERT}}$ or $k_L a$ [18]. Transport through an electrode membrane can be described by Eq. (2) [18].

$$\frac{dC_p}{dt} = \frac{1}{\tau_p}(C_L - C_p) \quad (2)$$

In order to determine τ_p , the DO probe was immersed in a bath purged with nitrogen and then quickly transferred to an oxygen saturated bath, both of which were maintained at 30 °C by the use of a water bath. The probe response was measured several times throughout the duration of the experiment and τ_p was found to be approximately $18.9 \text{ s} \pm 1.01 \text{ s}$. This response is higher than expected from both the literature [19], as well as the probe manual [20], and may be due to the age of the probe. Eq. (2) was solved simultaneously with Eq. (1) in order to produce a second order approximation to describe the experimental data considering the probe response. From this approximation the actual $k_L a_{\text{eff}}$, $k_L a_{\text{INERT}}$ or $k_L a$ was determined.

2.2. Oxygen uptake by the polymer phase

Transport in series is a common model used for a gas–liquid system containing suspended solids larger than the liquid film thickness between the gas and liquid phases [21]. This involves oxygen mass transfer occurring between the gas and liquid as well as between the liquid and solid, which is represented in Fig. 1. For this model, the effects of particles on gas–liquid mass transfer must be considered. In addition, as can be seen in Fig. 1, the absorptive effects of the particles will have an impact on the measured $k_L a_{\text{eff}}$ for particles with a considerable oxygen diffusion coefficient. For polymers with a significantly

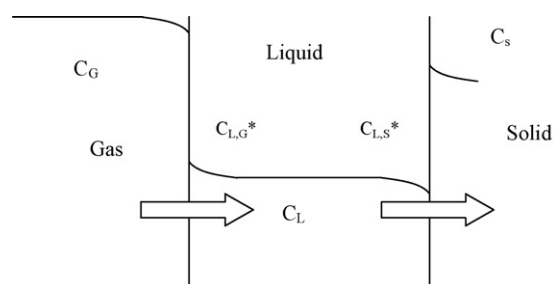


Fig. 1. Transport in a three phase system with large particles.

high oxygen diffusion coefficient, transport of oxygen into the liquid phase can be expressed using Eq. (3).

$$\frac{dC_L}{dt} = E_p k_L a (C^* - C_L) - \frac{dC_S}{dt} \left(\frac{V_S}{V_L} \right) \quad (3)$$

where the physical enhancement term, E_p , is defined using Eq. (4).

$$E_p = \frac{k_L a_{\text{INERT}}}{k_L a} \quad (4)$$

Therefore, for systems with inert polymers, oxygen transport in the liquid phase can be described using Eq. (5).

$$\frac{dC_L}{dt} = E_p k_L a (C^* - C_L) = k_L a_{\text{INERT}} (C^* - C_L) \quad (5)$$

Density and radius have been identified as critical properties to physical enhancement, and it is therefore possible to choose inert and absorptive particles that will yield the same E_p . Therefore, E_p can be estimated from Eq. (4), and used in Eq. (3). This allows for nylon 6,6 oxygen data (virtually no oxygen absorption into the polymer) to be used in Eq. (4) to estimate E_p to be used in Eq. (3) for the silicone rubber system. The same could be done to estimate an E_p for the styrene–butadiene copolymer system, however this was not completed due to the inability to locate inert polymers with the proper density and radius.

In order to determine the oxygen uptake by polymers, Eq. (3) can be rearranged to give Eq. (6).

$$\frac{dC_S}{dt} = \frac{V_L}{V_S} \left[E_p k_L a (C^* - C_L) - \frac{dC_L}{dt} \right] \quad (6)$$

An estimation of dC_L/dt can be obtained using an Euler approximation for each data point collected for oxygen concentration in the liquid phase as a function of time. The oxygen concentration in the liquid phase that was recorded for each time can also be substituted in Eq. (6) and an instantaneous oxygen uptake rate into the silicone rubber polymers can be calculated as a function of time. In MATLABTM, a spline was fit to the resulting plot of dC_S/dt versus time, which was integrated in MATLABTM using the trapezoidal rule in order to determine the total mass of oxygen taken up by the silicone rubber polymers. This was completed for 0.5, 0.75 and 1 L/min at an agitation rate of 400 rpm for data between 30% and 80% of liquid saturation.

2.3. System oxygen transfer rate

The concentration of oxygen in the working volume, C_{sys} , is defined as the sum of the concentration of oxygen in the liq-

uid phase and the concentration of oxygen in the solid phase. Oxygen transport into the working volume of the liquid–solid system can be expressed by Eq. (7).

$$(V_S + V_L) \frac{dC_{\text{sys}}}{dt} = V_L \frac{dC_L}{dt} + V_S \frac{dC_S}{dt} \quad (7)$$

Substituting Eq. (3) into Eq. (7) yields Eq. (8).

$$(V_S + V_L) \frac{dC_{\text{sys}}}{dt} = V_L \left(E_p k_L a (C^* - C_L) - \frac{dC_S}{dt} \left(\frac{V_S}{V_L} \right) \right) + \frac{dC_S}{dt} V_S \quad (8)$$

which reduces to Eq. (9).

$$\frac{dC_{\text{sys}}}{dt} = \frac{V_L}{(V_S + V_L)} (E_p k_L a (C^* - C_L)) \quad (9)$$

This allows for the instantaneous calculation of the oxygen transfer rate into the system, dC_{sys}/dt . Again, a spline was fit and integrated in MATLAB™, in order to determine the total mass

of oxygen transferred into the system. A dynamic period was used to determine the oxygen transfer rate into the system to be consistent with the reduction in oxygen limiting conditions in a solid–liquid TPPB that was observed in previous work [2]. The reduction occurred during transient steps in substrate concentration, which caused large oxygen uptake rates by the cellular population. Therefore, dynamic absorption rates are useful to simulate this situation.

3. Results and discussion

3.1. Volumetric mass transfer coefficients

The volumetric mass transfer coefficients for aqueous systems containing nylon 6,6, styrene–butadiene copolymer, silicone rubber, and tap water without particles are shown in, respectively, Fig. 2a–d. The $k_{L,a_{\text{eff}}}$ values are up to 55% lower for the system with styrene–butadiene relative to the system without particles and up to 63% lower for the system containing

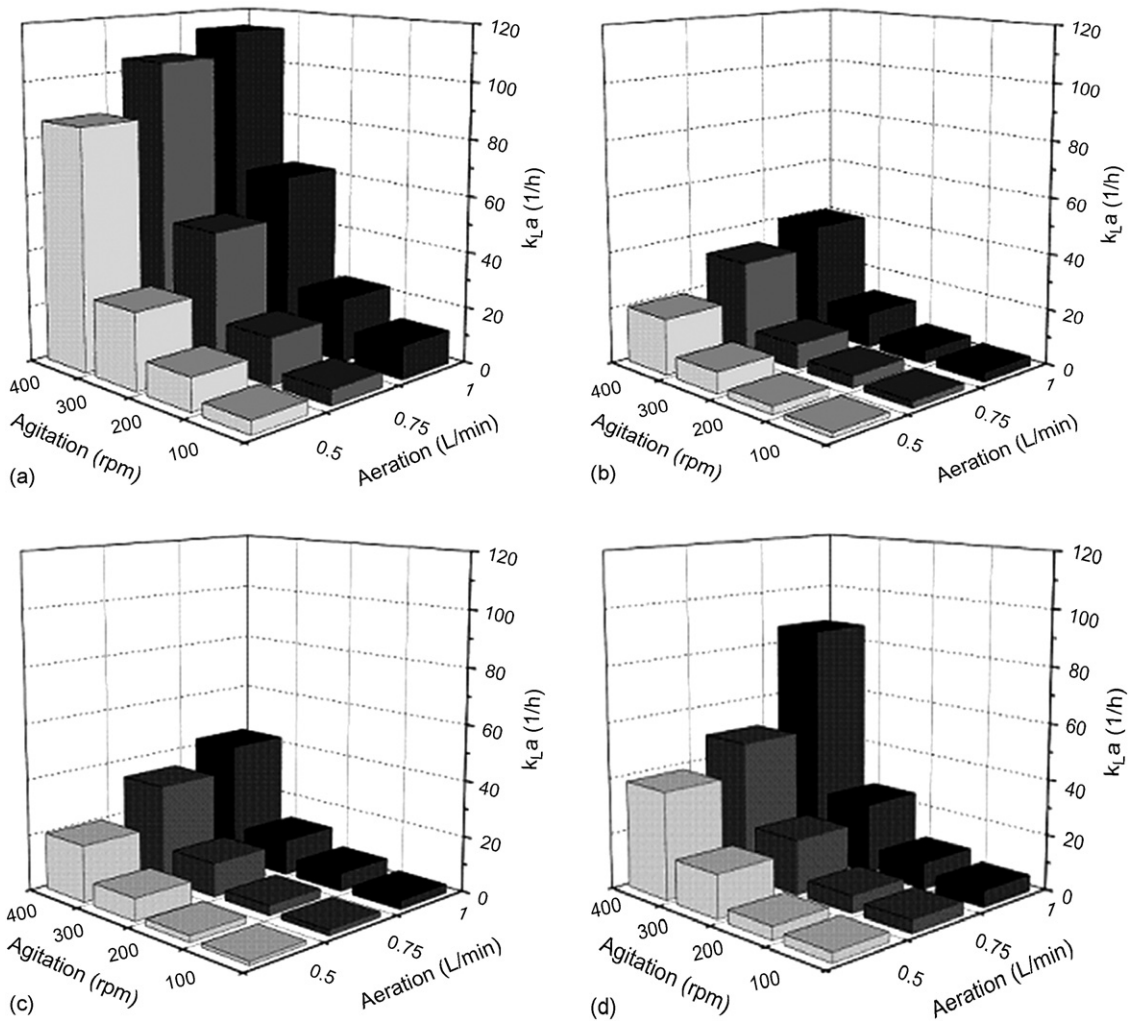


Fig. 2. (a) Inert volumetric mass transfer coefficients for an aqueous system containing 500 g nylon 6.6. (b) Effective volumetric mass transfer coefficients for an aqueous system containing 500 g styrene–butadiene copolymer. (c) Effective volumetric mass transfer coefficients for an aqueous system containing 500 g silicone rubber. (d) Volumetric mass transfer coefficients for an aqueous system containing no polymers.

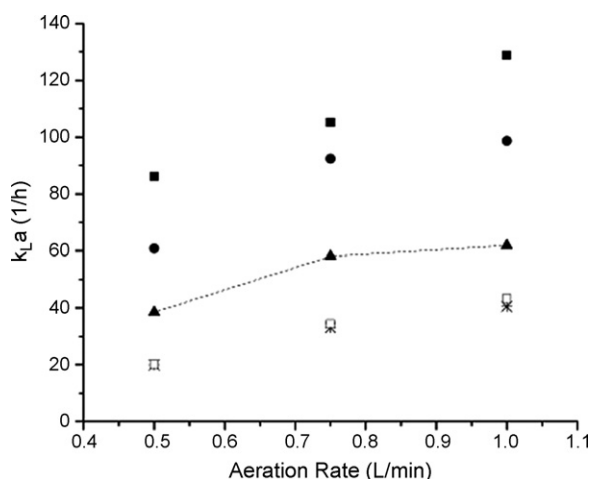


Fig. 3. Effective volumetric mass transfer coefficients at 400 rpm for nylon 6,6 (square), glass beads (circle), water (triangle and line), silicone rubber (open square) and styrene-butadiene copolymer (star).

silicone rubber. For systems containing styrene-butadiene copolymer and silicone rubber, the measurement of $k_{L}a_{\text{eff}}$ contains the effect of the solid polymer absorbing oxygen, as well as any effects the particles may have on gas-liquid mass transfer. The system containing nylon 6,6 shows up to a 268% increase in $k_{L}a_{\text{eff}}$ relative to $k_{L}a$. Due to the low oxygen diffusion coefficient of nylon 6,6, the effect of the particles on the gas-liquid mass transfer coefficient is isolated, and mass transfer enhancement is clearly observed. For all systems at lower operating conditions, $k_{L}a_{\text{eff}}$, $k_{L}a_{\text{INERT}}$ and $k_{L}a$ increases with both agitation and aeration rates. This increase with agitation and aeration has been documented in many other systems containing a second phase [1,4,7].

Fig. 3 clearly displays $k_{L}a_{\text{eff}}$, $k_{L}a_{\text{INERT}}$ and $k_{L}a$ for different aeration rates at 400 rpm for each solid type, including glass beads, and for the water-only system. In a similar manner to nylon 6,6, glass beads are inert and enhance the gas-liquid mass transfer up to 159%. These results are in agreement with findings that describe an increase in $k_{L}a$ in an external loop airlift reactor containing glass beads of 2.3 mm diameter [4]. Fig. 3 also shows that the enhancement of the gas-liquid mass transfer is much larger for the system containing nylon 6,6 than for the system containing glass beads. Other authors have found that an increase in solid density results in a decrease in $k_{L}a$, and this is a possible explanation for a denser solid type, glass, having a smaller $k_{L}a_{\text{INERT}}$ than a less dense solid type, nylon 6,6 [6]. Silicone rubber and styrene-butadiene have very similar decreases in $k_{L}a_{\text{eff}}$ relative to $k_{L}a$. A study completed on biomass support particles made from Scotchbrite™ pads of volumes 0.1625, 0.65 and 1.4625 cm³ also reported a similar decrease in $k_{L}a_{\text{eff}}$. This decrease was attributed to be a result of a coalescence process, as well as occupation of the liquid volume by the biomass support particles decreasing the effective interfacial area [7].

It can be seen from Table 1 that both nylon 6,6 and silicone rubber have very similar dimensions and densities, which have been identified earlier as critical factors for the effect of par-

ticles on gas-liquid mass transfer. Nylon 6,6, can therefore be used to approximate the effect of silicone rubber on gas-liquid mass transfer, as both the effects of oxygen absorption by the silicone rubber and the effects on the gas-liquid mass transfer are contained within the measured $k_{L}a_{\text{eff}}$ for the silicone rubber system and cannot be separated. At an agitation rate of 400 rpm, nylon 6,6 resulted in enhancement factors for 0.5, 0.75 and 1 L/min, of, respectively, 2.23, 1.81 and 1.83, which should also be the approximate effects of silicone rubber on gas-liquid mass transfer. These enhancement approximations may contain error due to the assumption that particle hydrophobicity effects can be neglected. Hydrophobicity, or wettability, of the particles has been shown to be a critical property on gas-liquid mass transfer [13]. However, due to the assumption that the system is well mixed, the interactions of the particles with the gas-liquid interface are not increased for a hydrophobic particle, but are equal for all particle types as the particles are evenly distributed throughout the system.

At larger agitation and aeration rates, $k_{L}a_{\text{eff}}$, $k_{L}a_{\text{INERT}}$ and $k_{L}a$ were also measured for systems containing silicone rubber, styrene-butadiene copolymer, nylon 6,6 and water without solids (data not shown). Again, $k_{L}a_{\text{eff}}$, $k_{L}a_{\text{INERT}}$ and $k_{L}a$ increased with aeration rate for each system in a similar fashion as it did at the lower operating conditions. However, all systems, with the exception of silicone rubber, revealed an increase in $k_{L}a_{\text{eff}}$ and $k_{L}a_{\text{INERT}}$ relative to $k_{L}a$ at large agitation rates. This may be attributed to the oxygen uptake by the polymers not being observable, as it is possible that oxygen was transferred from the gas to the liquid at such a fast rate that the liquid was saturated before significant amounts of oxygen could be taken up by the polymer beads. The data for high agitation and aeration rates also revealed that there appears to be an optimum agitation rate of 600 rpm for the liquid-polymer systems, as the measurements at 800 rpm showed a decrease in $k_{L}a_{\text{eff}}$ and $k_{L}a_{\text{INERT}}$. This decrease is likely due to a hydrodynamic effect that is unknown; operating zones with inconsistent behavior have been noted in other oxygen mass transfer experiments [1]. One author reported an increase in stirrer speed caused a plateau effect in the $k_{L}a$ in a gas-liquid-solid system with activated carbon at higher agitation rates [3].

3.2. Oxygen uptake by the polymer phase

The instantaneous oxygen uptake rate by silicone rubber beads was calculated using Eq. (6). A plot of the instantaneous oxygen uptake rate versus time was then integrated in order to determine the mass taken up by the polymer between 30% and 80% of liquid saturation. The mass of oxygen taken up by silicone rubber at an agitation rate of 400 rpm is shown in Fig. 4 for aeration rates of 0.5, 0.75 and 1 L/min. A larger amount of oxygen is taken up by the system aerated at 0.5 L/min than systems at 0.75 and 1 L/min. This result is expected, as silicone rubber has a longer time to take up oxygen if the liquid phase takes longer to saturate. It is expected that the system aerated at 0.75 L/min will take up more oxygen between 30% and 80% of liquid saturation than the 1 L/min system, however, a significant difference was not seen in the data. These results

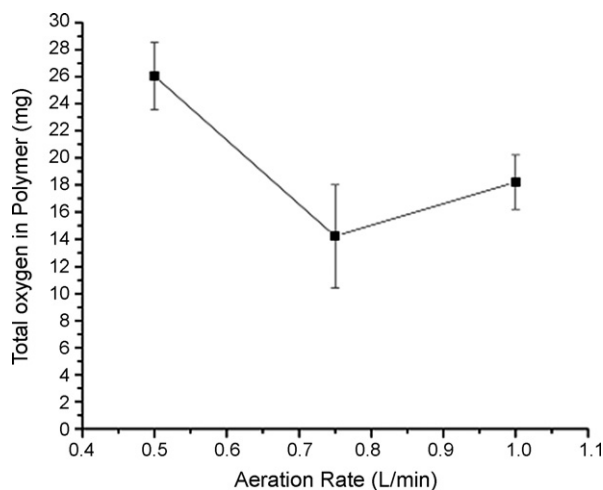


Fig. 4. Total amount of oxygen taken up by silicone rubber during a period between 30% and 80% of saturation of the liquid phase.

suggest that silicone rubber takes up a considerable amount of oxygen at a rate that is observable during the dynamic period of liquid saturation by gas sparging for lower operating conditions. These results shed light on previous findings in our laboratory [2] involving styrene–butadiene copolymer in a TPPB providing oxygen during what would otherwise be oxygen limiting conditions in the aqueous phase, as mass transfer between the polymer and aqueous phases is sufficiently fast.

3.3. System oxygen transfer rate

In order to demonstrate a larger overall uptake of oxygen into a TPPB system relative to a system without a second phase, Eq. (9) was utilized. The instantaneous oxygen transfer rate as a function of time at 400 rpm agitation and 1 L/min aeration for a solid–liquid system containing silicone rubber beads is shown in Fig. 5. Also shown in Fig. 5 is the instantaneous oxygen

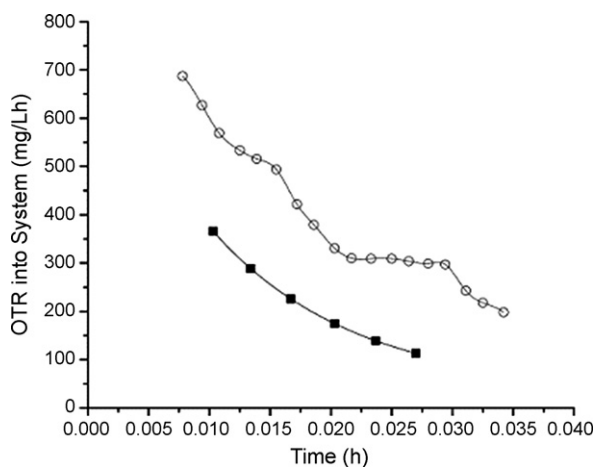


Fig. 5. Oxygen transfer rate as a function of time between 30% and 80% of liquid saturation by a system of water with silicone beads (open circles) and water without particles (closed squares) and splines fitting both trends (lines).

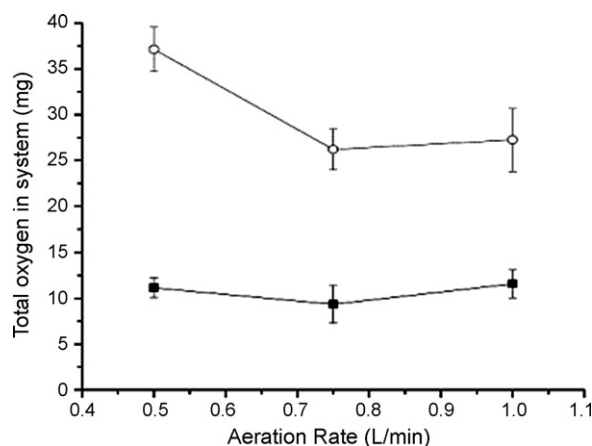


Fig. 6. Total oxygen transferred into the system between 30% and 80% of liquid saturation for a system of silicone in water (open circles) and water without particles (squares).

transfer rate as a function of time for a system without a second phase, which was calculated using Eq. (1). This plot clearly shows that between 30% and 80% of liquid saturation the system containing silicone rubber beads has a much larger oxygen transfer rate during the progression to liquid saturation than the system without a second phase. As well, the system with a second phase reaches 80% liquid saturation much later than the system without a second phase. This is due to the polymers acting as an oxygen sink within the system, in turn causing the liquid oxygen concentration to be lower relative to the system without polymers, at any given time. This decrease in the liquid concentration causes an increased driving force for oxygen between the gas and liquid phases, which causes a larger oxygen transfer rate for an extended period of time. Therefore, although the $k_L a_{\text{eff}}$ is measured as lower for the reasons explained previously, the overall oxygen transfer rate into the solid–liquid system is larger. This is due to the oxygen transfer rate not only being proportional to the volumetric mass transfer coefficient, but also to the increased instantaneous concentration driving force.

The curves shown in Fig. 5 were also obtained at 400 rpm for aeration rates of 0.5 and 0.75 (data not shown). These curves were integrated in order to determine the total mass of oxygen transferred into the working volume for both a system containing an absorptive polymer and a system without polymers, which can be seen in Fig. 6. More than twice the total oxygen was transferred into the system containing silicone rubber beads than the system without polymers from 30% to 80% of liquid saturation. The polymers have a large uptake of oxygen and therefore more oxygen can ultimately be contained within the system. These results are comparable to those for liquid–liquid systems that have found that oxygen is transferred at a higher rate due to an increased driving force [1]. However liquid–liquid systems can be viewed as increasing the working volume oxygen saturation concentration, whereas the solid–liquid system increases the driving force by decreasing the liquid concentration at any given time, as well as by possibly enhancing gas–liquid mass transfer. Nevertheless,

both liquid–liquid and solid–liquid systems increase the overall amount of oxygen that can be contained within a working volume.

Also shown in Fig. 6 is a decrease in the amount of oxygen transferred into the system containing silicone rubber as aeration rate increases. At higher aeration rates the required time for the liquid phase to saturate decreases. This may cause the polymers to have a shorter period of time to absorb oxygen and the total mass of oxygen observed to be transferred into the system between 30% and 80% of liquid saturation will decrease. It can be seen that the system without a second phase has a relatively constant total amount of oxygen transferred into the system between 30% and 80% of liquid saturation, as no oxygen sink exists.

This observed enhanced oxygen uptake into the system due to the presence of solid particles has positive implications on many aerobic fermentations. Oxygen limitations within a cell-containing liquid phase can be reduced by transfer occurring to the liquid phase from a solid phase with a large oxygen capacity in order to maintain thermodynamic equilibrium. This concept has been demonstrated for several liquid–liquid systems that contain “oxygen carriers”, a liquid phase with a higher oxygen solubility than water. One study involved the use of a bioreactor containing liquid Poly(dimethylsiloxane) (PDMS) as an oxygen carrier for the application of wood bleaching. PDMS was used to improve oxygen availability to the white rot fungus *Trametes versicolor*. This study displayed that the addition of 0.5% PDMS caused a significant improvement in the whitening of pulp, as well as the production of biomass, relative to a control with no oxygen carriers present [22].

4. Conclusions

For the solid types tested in an abiotic TPPB, relative to a system without a second phase, the $k_L a_{\text{eff}}$ was measured to be lower when containing styrene–butadiene copolymer as well as silicone rubber, and $k_L a_{\text{eff}}$ was measured to be higher for the systems containing nylon 6,6 and glass beads. The reason for this deviation was attributed to the effect of particles on gas–liquid mass transfer for all systems, as well as an oxygen absorption effect for systems containing polymers with high oxygen diffusivity.

The proposed transport in series model, which combines the effect of gas–liquid mass transfer enhancement with oxygen absorption by the particle, allows for the calculation of the rate of oxygen transfer into the solid material. However, this calculation is reliant upon the assumption that the working volume is well mixed and particle hydrophobicity will not increase interactions with gas–liquid interface, and therefore will not increase enhancement.

Finally, it was shown that the overall oxygen transfer rate for a system containing silicone rubber beads was more than double the oxygen transfer rate of a system without polymers during 30–80% of the liquid saturation. This clarifies our previous results regarding the presence of styrene–butadiene copolymer particles as the second phase in a TPPB reducing oxygen limitations. As well, implications from this study can be applied

to many solid–liquid aerobic fermentations with regard to their ability to avoid oxygen limiting conditions.

Acknowledgement

The financial support of the Natural Science and Engineering Research Council of Canada is gratefully acknowledged.

References

- [1] D.R. Nielsen, A.J. Daugulis, P.J. McLellan, A Restructured framework for modeling oxygen transfer in two-phase partitioning bioreactors, *Biotechnol. Bioeng.* 91 (6) (2005) 773–777.
- [2] N.G. Boudreau, A.J. Daugulis, Transient performance of two-phase partitioning bioreactors treating a toluene contaminated gas stream, *Biotechnol. Bioeng.* 94 (3) (2006) 448–457.
- [3] J.H.J. Kluytmans, B.G.M. van Wachem, B.F.M. Kuster, Mass transfer in sparged and stirred reactors: influence of carbon particles and electrolyte, *Chem. Eng. Sci.* 58 (20) (2003) 4719–4728.
- [4] Y.X. Guo, M.N. Rathor, H.C. Ti, Hydrodynamics and mass transfer studies in a novel external-loop airlift reactor, *Chem. Eng. J.* 67 (3) (1997) 205–214.
- [5] J.T. Tinge, A.A.H. Drinkenburg, The enhancement of the physical absorption of gases in aqueous activated carbon slurries, *Chem. Eng. Sci.* 50 (6) (1995) 937–942.
- [6] C. Freitas, J.A. Teixeira, Oxygen mass transfer in a high solids loading three-phase internal-loop airlift reactor, *Chem. Eng. J.* 84 (1) (2001) 57–61.
- [7] B. Özbek, S. Gayik, The studies on the oxygen mass transfer coefficient in a bioreactor, *Process Biochem.* 36 (8–9) (2001) 729–741.
- [8] N.C. Gogoi, N.N. Dutta, Empirical approach to solid–liquid mass transfer in a three-phase sparged reactor, *Fuel Process. Technol.* 48 (2) (1996) 145–157.
- [9] R.V. Roman, R.Z. Tudose, Studies on transfer processes in mixing vessels: effect of particles on gas–liquid mass transfer using modified rushton turbine agitators, *Bioprocess Eng.* 17 (6) (1997) 361–365.
- [10] G.D. Zhang, W.F. Cai, C.J. Xu, A general enhancement factor model of the physical absorption of gases in multiphase systems, *Chem. Eng. Sci.* 61 (2) (2006) 558–568.
- [11] S.S. Öztürk, A. Schumpe, The influence of suspended solids on oxygen transfer to organic liquids in a bubble column, *Chem. Eng. Sci.* 42 (7) (1987) 1781–1785.
- [12] A.A.C.M. Beenackers, W.P.M. Van Swaaij, Mass transfer in gas–liquid slurry reactors, *Chem. Eng. Sci.* 48 (18) (1993) 3109–3139.
- [13] A. Schumpe, A.K. Saxena, K.D.P. Nigam, Gas/liquid mass transfer in a bubble column with suspended nonwetttable solids, *AIChE J.* 33 (11) (1987) 1916–1920.
- [14] O. Ozkan, A. Calimli, R. Berber, Effect of inert solid particles at low concentrations on gas–liquid mass transfer in mechanically agitated reactors, *Chem. Eng. Sci.* 55 (14) (2000) 2737–2740.
- [15] R.L. Kars, R.J. Best, A.A.H. Drinkenburg, The sorption of propane in slurries of active carbon in water, *Chem. Eng. J.* 17 (3) (1997) 201–210.
- [16] K.C. Ruthiya, J. van der Schaaf, B.F.M. Kuster, Mechanisms of physical and reaction enhancement of mass transfer in a gas inducing stirred slurry reactor, *Chem. Eng. J.* 96 (1–3) (2003) 55–69.
- [17] M.L. Shuler, F. Kargi, *Bioprocess Engineering*, 2nd ed., Prentice Hall, New Jersey, 2002.
- [18] W.A. Brown, Developing the best correlation for estimating the transfer of oxygen from air to water, *Chem. Eng. Educ.* 35 (2) (2001) 134–147.
- [19] D.R. Nielsen, A.J. Daugulis, P.J. McLellan, A novel method of simulating oxygen mass transfer in two-phase partitioning bioreactors, *Biotechnol. Bioeng.* 83 (6) (2003) 735–742.
- [20] Broadley James Corporation. Broadley and james model D100 series OxyProbe instruction manual (2000).
- [21] E. Alper, B. Wichtendahl, W.-D. Deckwer, Gas absorption mechanism in catalytic slurry reactors, *Chem. Eng. Sci.* 35 (1–2) (1980) 217–222.

- [22] E. Ziomek, N. Kirkpatrick, I.D. Reid, Effect of polydimethylsiloxane oxygen carriers on the biological bleaching of hardwood kraft pulp by *Trametes Versicolor*, *Appl. Microbiol. Biotechnol.* 35 (5) (1991) 669–673.
- [23] D. Jarus, A. Hiltner, E. Baer, Barrier properties of polypropylene/polyamide blends produced by microlayer coextrusion, *Polymer* 43 (8) (2002) 2401–2408.
- [24] W.J. Roff, J.R. Scott, J. Pacitti, Fibres, films, plastics and rubbers, in: *A Handbook of Common Polymers*, 1st ed., Butterworths, London, 1971.
- [25] T.C. Merkel, V.I. Bondar, K. Nagai, B.D. Freeman, I. Pinnau, Gas Sorption, Diffusion, and permeation in poly(dimethylsiloxane), *J. Polym. Sci., Part B: Polym. Phys.* 38 (3) (2000) 415–434.
- [26] J.D. Kalen, R.S. Boyce, J.D. Cawley, Oxygen tracer diffusion in vitreous silica, *J. Am. Ceram. Soc.* 74 (1) (1991) 203–209.